Int. J. Electrochem. Sci., 16 **(2021)** Article Number: 211054, doi: 10.20964/2021.10.43

International Journal of
ELECTROCHEMICAL
SCIENCE
www.electrochemsci.org

Effects of Solidification, Rotary Swaging and Recrystallization on the Microstructure, Crystallographic Orientation and Electrochemical Behavior of an Al-4.5 wt.% Cu Alloy

J.C. Lourenço[1,], L.P. Souza[1], G. Silva[2], P.A. Suzuki[1], A.L.M. Robin[1], C.A. Nunes[1], C.R. Tomachuk[1]*

[1] Universidade de São Paulo, Escola de Engenharia de Lorena – EEL/USP, Pólo-Urbo Industrial, Gleba AI-6, s/n, Lorena, SP, Brazil
[2] Universidade Federal de Itajubá, Itajubá, Minas Gerais, Brazil.
[*]E-mail: julio.lourenco@usp.br

Received: 23 February 2021 / *Accepted:* 7 July 2021 / *Published:* 10 September 2021

The evolution of the microstructure and grain orientation of metallic alloys during plastic deformation and recrystallization is of particular interest because these characteristics are known to strongly affect their mechanical properties and corrosion resistance. In this work, the hypoeutectic Al-4.5 wt.% Cu alloy was produced under conventional and vertical upward unidirectional solidification, followed by rotary swaging with 54%, 76% and 91% degrees of deformation and recrystallization treatment at 350 °C for 60 min. The microstructure of the as-cast alloy obtained by conventional solidification presented an equiaxed morphology, whereas that obtained by directional solidification was columnar. Rotary swaging led to gradual grain elongation, a decrease in interdendritic arm spacing and eutectic microsegregation. Recrystallization treatment changed the microstructure to an equiaxed morphology. The as-cast alloy obtained by conventional and unidirectional solidification routes presented the (111) and (200) preferred orientations, respectively. These preferred orientations gradually disappeared with plastic forming by rotary swaging, which was changed to the (220) preferred orientation in both cases as the deformation increased. A randomly oriented grain microstructure was obtained after recrystallization treatment. Under conventional solidification conditions, the as-cast sample exhibited better corrosion resistance. On the other hand, in the vertical upward unidirectional solidification condition, the deformed 91% recrystallized sample presented nobler behavior, while the as-cast sample presented lower corrosion resistance. Higher reductions promoted a reduction in the corrosion resistance of both solidification conditions. Changes in the crystallographic orientation promoted differences in the corrosion resistance.

Keywords: Al-Cu alloy, solidification, swaging, microstructure, texture

1. INTRODUCTION

In recent decades, aluminum alloys have been used in several applications, such as in the aerospace, automotive, marine, packaging and construction industries, playing a significant role in

modern society [1]. Copper is an element usually added to aluminum to improve its mechanical properties and machinability. The usual Al-Cu alloys contain from 4% to 10% copper [1]. Nevertheless, copper addition generally leads to a decrease in general corrosion, intergranular corrosion and stress corrosion cracking resistances due to the presence of cathodic intermetallic Al_2Cu particles, which create galvanic cells with a less noble Al-rich phase [2].

Although extensive literature on Al-Cu systems has been produced, the effects of casting methods, plastic forming and recrystallization on the microstructure, crystallographic orientation and corrosion behavior of alloys in aqueous solutions have not been well documented and are dispersed among several studies. Additionally, it seems that no correlation between microstructures, textures and corrosion behavior has been proposed for this system.

Henry et al. [3] showed that the mode of solidification affects the shape of the grains. Conventional solidification, for example, starts at the wall of the mold and progresses perpendicularly from that surface to the center, and the macrostructure will be composed of a thin external chill layer, an intermediary columnar layer and a great central equiaxed zone. During vertical upward unidirectional solidification, chilling occurs at the bottom of the cast, which results in a small chill zone in contact with the cold wall, a large columnar vertically oriented zone, and an equiaxed region at the top.

Regarding the solidification process, Xie et al. [4] schematically described the variation in the microstructure of an Al-Cu alloy with time during directional solidification for different cooling rates. Eskin et al. [5] used different techniques of solidification of Al-Cu and showed that increasing the cooling rate and copper content led to a refinement of the grain structure and a decrease in dendrite arm spacing.

Osório et al. [6] studied the corrosion behavior in NaCl solution of equiaxed and columnar structures of Al-5 wt.% Cu and Al-8 wt.% Cu alloys obtained by vertical upward unidirectional solidification and attributed the same resistance observed in these alloys to similar secondary dendrite arm spacings in both zones. Osório et al. [7] reported lower corrosion resistance in Al-Cu alloys with coarser dendritic structures provided by low cooling rates.

Robin et al. [8] reported that phase transformations can be induced by plastic deformation, affecting important microstructural characteristics, such as grain size and shape, dislocation density and texture. Moreover, these changes can modify the properties of the materials.

Padilha and Siciliano-Jr [9] claimed that forming aluminum wires by cold drawing leads mostly to the (111) texture. Engler et al. [10] reported that during rolling, the initial cube orientation (001) [100] of Al-1.8 wt.% Cu crystals was retained for thickness reduction up to 63%. At 78% reduction, the single cube orientation was decomposed, and at a high deformation degree of 95%, the four variants of the texture S-orientation were clearly evidenced. Engler et al. [11] also studied the influence of recrystallization treatment at different temperatures and times on Al-1.8 wt.% Cu crystals with Goss, brass and copper initial orientations rolled with a reduction degree of approximately 90% and provided an interpretation of the recrystallization textures of the different crystals. Abdulstaar et al. [12] showed that the ultrafine-grained commercial AA1050 alloy deformed by rotary swaging is more corrosion-resistant in NaCl solutions than the coarse-grained as-received alloy, which is the result of a denser and more stable passive film produced on forged metal.

The present study aims to identify the effects of the production of hypoeutectic Al-4.5 wt.% Cu alloy under conventional or vertical directional solidification, followed by rotary swaging and recrystallization treatment regarding their microstructure and crystallographic orientation. The influence of the degree of deformation during cold forging was investigated. Electrochemical measurements were performed and correlated with microstructure to understand the effects that crystallographic effects and deformation have on this alloy.

2. EXPERIMENTAL PROCEDURE

Samples of Al-4.5 wt.% Cu alloy were received under the conditions shown in Table 1. The first route of production (conventional solidification) consisted of melting commercially pure aluminum and commercially pure copper in the proportions of the alloy in an electric furnace at 750 °C for 1 h, casting the liquid alloy in a cylindrical mold of 18 mm internal diameter, and then machining the ingot to a 15 mm final diameter, as described by Matos [13]. The second route (vertical upward unidirectional solidification) of alloy manufacturing was through a water-cooled vertical upward unidirectional solidification system. The wall of the crucible was thermally isolated, and the heat was only extracted through the water-cooled bottom. The solidified ingot of 38 mm diameter was also machined to obtain a rod of 15 mm final diameter. Both rods were cold-swaged using a rotary swaging FENN machine. In the swaging process, the initial samples (rods) were slid into three dies that open and close rapidly to provide the impact action that shapes the workpiece through plastic deformation. While the dies and the rod are in contact, the workpiece is also forced to rotate on its axis. As the rotation speed of the dies is higher than the rotation of the rod, the rod is hit in different positions by the dies, and the final workpiece is a round section with a smaller diameter than it was before the process.

Table 1. Samples of Al-4.5%wt. Cu alloy as-received

Samples	**Degree of deformation by rotary swaging (%)**	
	Conventional solidification	**Vertical upward unidirectional solidification**
as-cast	0	0
54%	54	54
76%	76	76
91%	91	91
91%RC	91 - Recrystallized	91 - Recrystallized

Samples with diameters of 10.2 mm, 7.4 mm and 4.7 mm were collected, which correspond to 54%, 76% and 91% of the deformation degree, respectively. Heat treatment at 350 °C for 60 min in an EDG 3P-S furnace and cooling in air were performed on rods swaged up to 91% of the deformation

degree to achieve full recrystallization. Matos [13] gives full details on the solidification, swaging and recrystallization processes. The rods were cut along the longitudinal direction at the middle (solidification and cold-working directions), and the sectioned faces were ground with SiC abrasive papers to a 2600 grit finish and polished using a 0.4 μm colloidal silica suspension solution.

For the analysis of microstructures by light optical microscopy (LOM), a Leica DM4000 M model optical microscope and a Hitachi TM3000 series scanning electron microscope (SEM) were used. Samples were grounded with #2400 SiC paper and etched by Keller reagent (90 ml distilled water + 2 ml HF (48%) + 3 ml HCl (37%) + 5 ml HNO_3 (65%)).

The same but not etched samples were used for analyses by X-ray diffractometry (XRD) in an Empyrean X-ray diffractometer from PANalatytical using Cu-Kα radiation. The measuring conditions were as follows: 10° to 90° angular range, 0.02° step and 15 s counting time. Five diffractograms and no sequential diffractograms were obtained for each sample, and the reproducibility of the results was ensured by the calculation of the standard deviations made on each identified phase peak. To obtain more accurate measurements, the samples were placed in the diffractometer chamber in a position where the grain solidification or conformation orientation was perpendicular to the X-ray beam. This procedure allowed the sweep of a larger number of grains, resulting in diffraction peaks of higher intensity. The device to hold the samples was made of PVC, which led to a single diffraction peak at 27°, and this peak was not coincident with any diffraction peak of the alloy.

To identify the diffraction peaks, PowderCell for Windows and Pearson's Crystal Data.Ink software were used. Additionally, crystallographic data compiled in Pearson's Crystal Data.Ink software for the Al-Cu alloys created Al-4.5 wt.% theoretical XRD patterns. For the texture analysis, the HighScore® program was used. The preferred orientation factor $R_{(h\,k\,l)}$ of an (*h k l*) plane was calculated for the studied samples according to the following formula proposed by Lotgering [14]:

$$R_{(hkl)} = \frac{I_{(hkl)}}{\sum I_{(hkl)}} \quad (1)$$

where $I_{(h\,k\,l)}$ corresponds to the integrated intensity of the (*h k l*) peak.

The orientation index $F_{(\mathrm{hkl})}$ of an (*h k l*) plane can be deduced from the relation:

$$F_{(hkl)} = \frac{R_{(hkl)}}{R_{0(hkl)}} \quad (2)$$

where $R_{(h\,k\,l)}$ is the preferred orientation factor calculated for the experimental diffractogram, and $R_{0(h\ k\ l)}$ is the preferred orientation factor calculated for the theoretical diffractogram of the alloy (corresponding to powder grains randomly oriented).

For the electrochemical measurements, samples were cold mounted in Bakelite and polished with #800 SiC paper. The electrochemical cell consisted of a three-electrode arrangement; the counter electrode (CE) was a Pt sheet (area of 12 cm^2), a saturated calomel electrode (SCE, Hg/Hg_2Cl_2, KCl_{sat}) was the reference electrode, and the sample was the working electrode (WE), defining an area of 1 cm^2. Measurements were performed at room temperature in 3.5 wt.% (0.6 M) NaCl solution.

The electrochemical measurement consisted of open circuit potential (OCP) vs. time over 3 h, followed by electrochemical impedance spectroscopy (EIS) measurements. The EIS measurements were performed in the frequency range between 10^{-2} Hz and 10^{5} Hz using a Solartron 1287S frequency response analyzer (FRA) in combination with a Solartron 1287 electrochemical interface and a superimposed sinusoidal voltage signal of 10 mV. The corrosion behavior was analyzed in triplicate.

After the EIS measurements, potentiodynamic polarization curves were obtained using a Solartron 1287A electrochemical system at a scan rate of 1 mVs^{-1} over the range –0.5 V/SCE to ≈ +0.2 V/SCE with respect to the corrosion potential. The corrosion current density and corrosion potential were obtained from a Tafel slope by extrapolation of the linear portion of anodic and cathodic branches.

3. RESULTS AND DISCUSSION

3.1. Microstructures

Figures 1a and 1b show the microstructures of the as-cast Al-4.5Cu wt.% alloy obtained by conventional and vertical upward unidirectional solidification methods, respectively. As predicted by the Al-Cu phase diagram, the microstructures are composed of two phases, the main phase composed of aluminum-rich α-Al with copper present in solid solution and a secondary Al_2Cu phase present along the interdendritic region, whose identification was made by X-ray diffractometry (see 3.2).

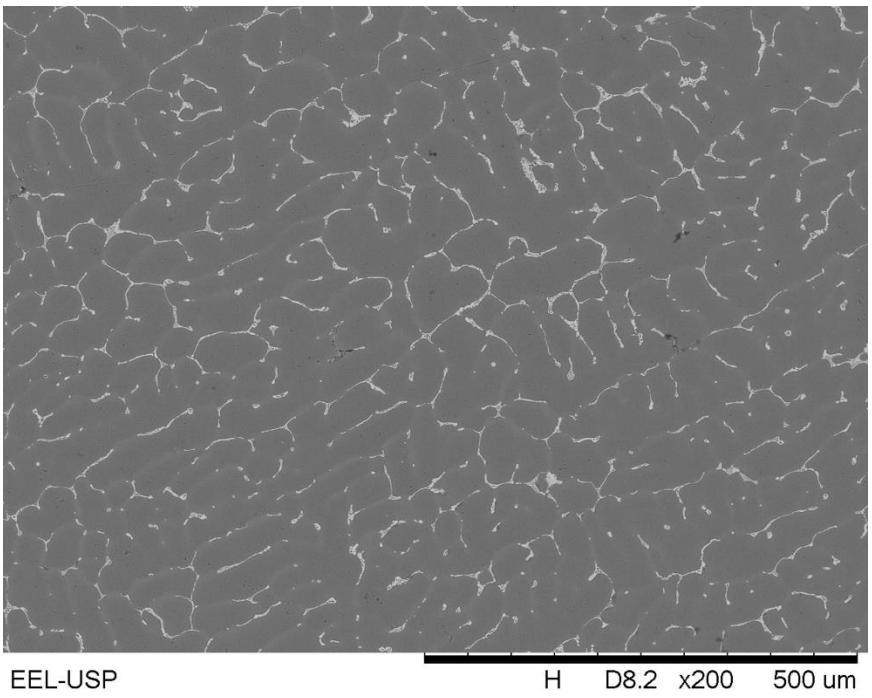

(a)

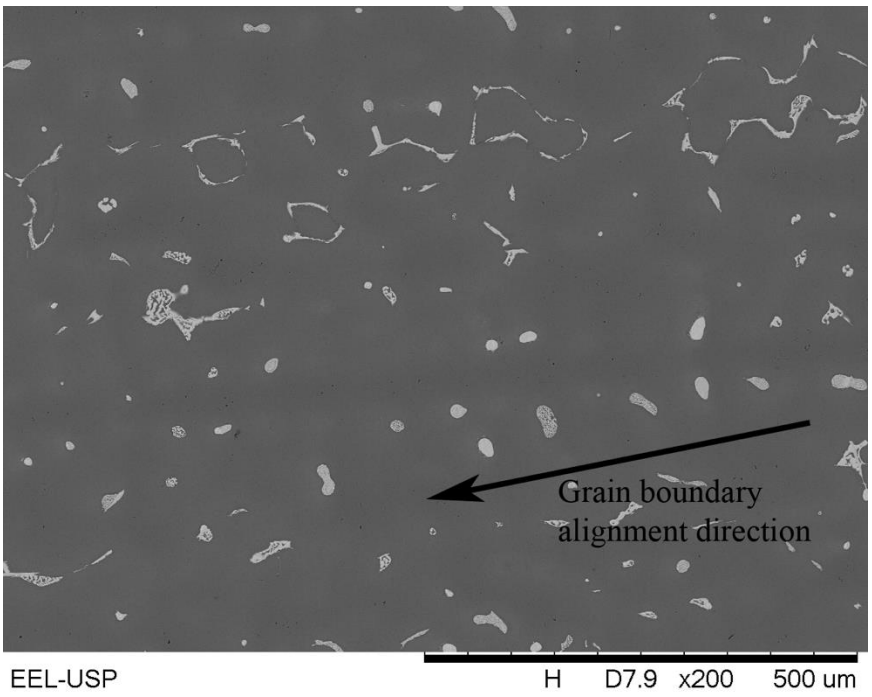

(b)

Figure 1. As-cast Al-4.5 wt.% Cu alloy microstructures obtained by (a) conventional and (b) vertical upward unidirectional solidification methods

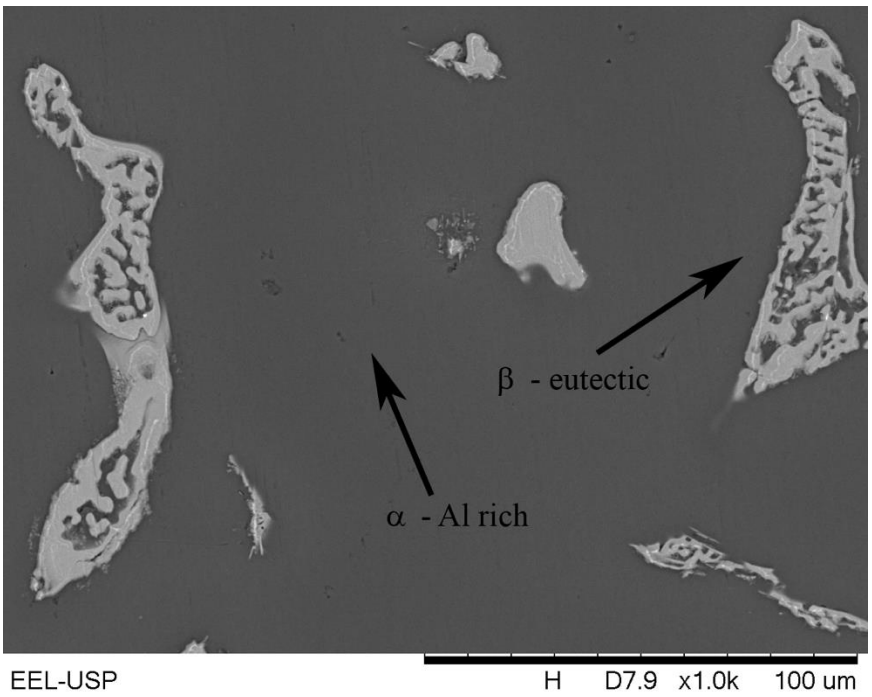

Figure 2. SEM micrograph of the as-cast Al-4.5 wt.% Cu alloy indicating the α-Al phase and β-eutectic in the matrix

According to Osório et al. [15], dendrites are formed of an α-Al phase composed of aluminum and copper in a substitutional solid solution, and the interdendritic region is a β-eutectic composed of α-Al and Al_2Cu lamellae (Figure 2). As expected, the microstructure of the as-cast Al-4.5Cu wt.% alloy obtained by conventional solidification presents an equiaxed morphology (Figure 1a). On the other hand, the microstructure obtained by directional solidification has a columnar morphology with the alignment of the grains in the direction of heat extraction (Figure 1b).

Rotary swaging led to the elongation of grains in the direction of plastic deformation and a decrease in the dendritic arm spacing with increasing deformation degree (Figure 3). Comparing the set of SEM images in Figure 3, it is possible to infer that for the same reduction in area, the interdendritic arm spacing is larger for the sample solidified unidirectionally.

As the reduction increased, the eutectic interdendritic constituent segregated more for both materials (Figure 4). This segregation occurred for the second phase, which did not withstand mechanical reduction as the α-Al-rich matrix. This is because Al_2Cu has a body-centered tetragonal lattice, which is known to have fewer active slip planes for deformation, while α-Al presents a face-centered cubic structure, known to have more active slip planes.

	Conventional solidification	Vertical upward unidirectional solidification
54%	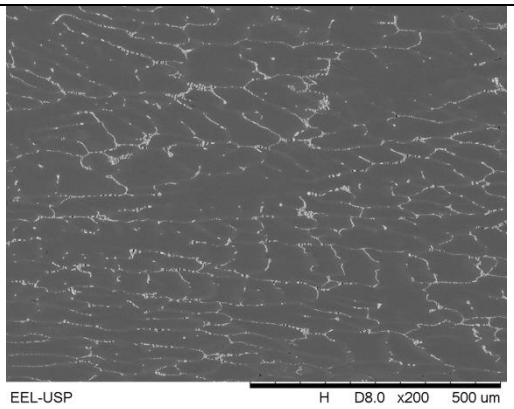	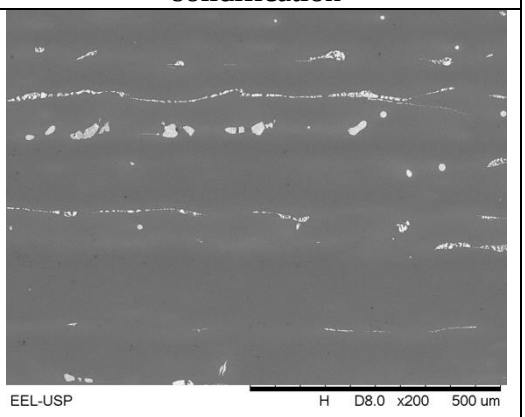
76%	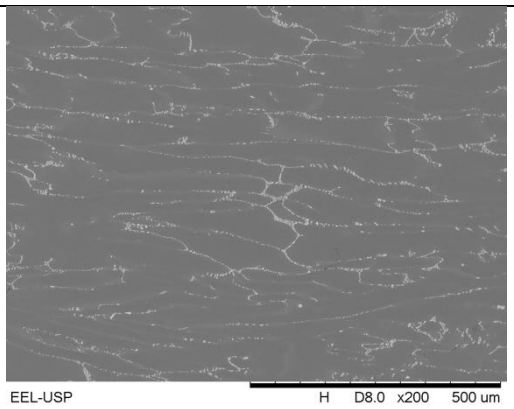	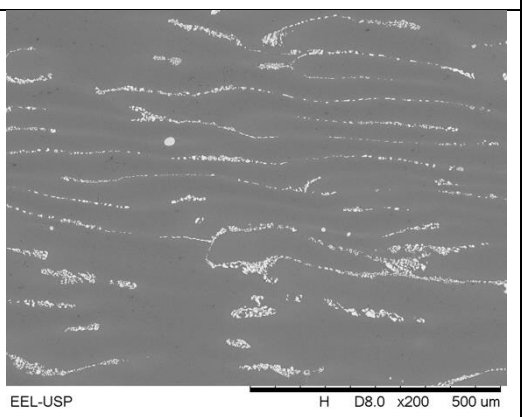

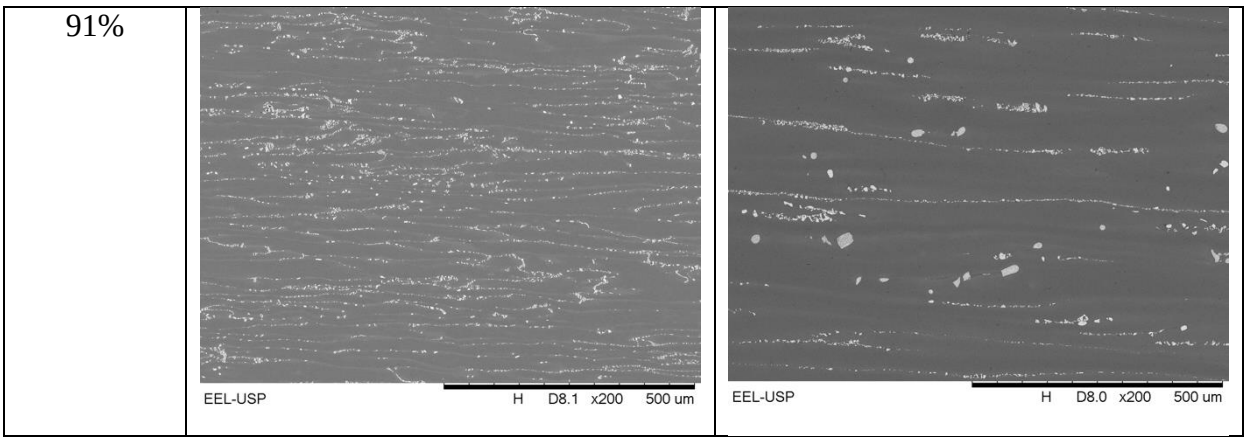

Figure 3. SEM micrographs of Al-4.5 wt.% Cu alloy after rotary swaging

Some cold-worked Al-4.5 wt.% Cu samples were submitted to heat treatment at 350 °C for 60 min for recrystallization. Figure 5 presents the SEM microstructure of the alloy obtained by the conventional solidification method, swaged up to a degree of deformation of 91% and recrystallized. The presence of a finely dispersed secondary phase can be identified in regions near the microsegregated Al_2Cu phase due to rotary swaging. The same occurred for the alloy obtained by the vertical upward unidirectional solidification route. The heat treatment provided the necessary energy for Al_2Cu partial aging, which was also facilitated by the high deformation degree of the samples [16].

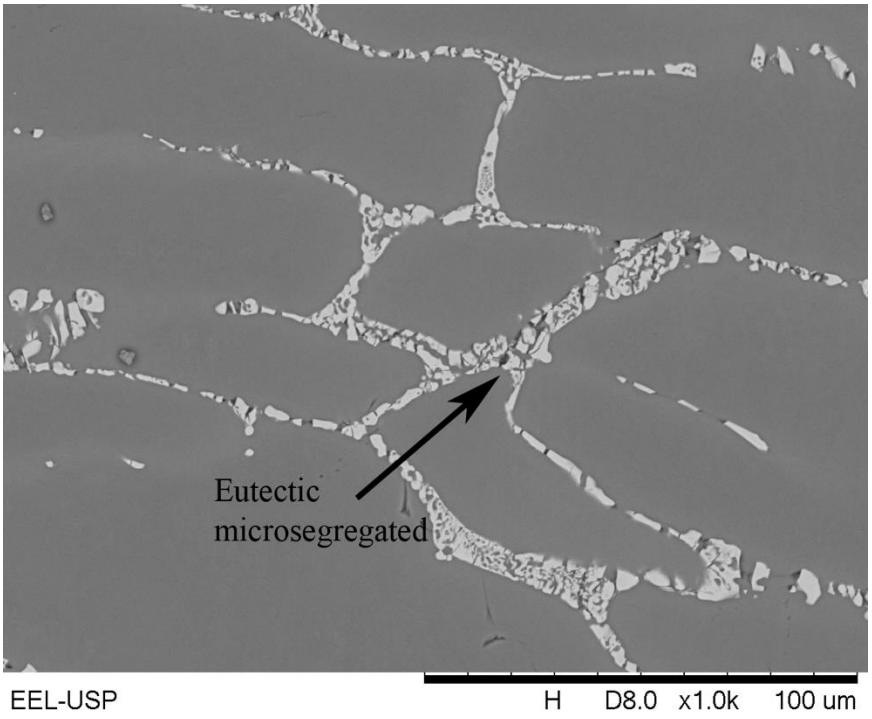

(a)

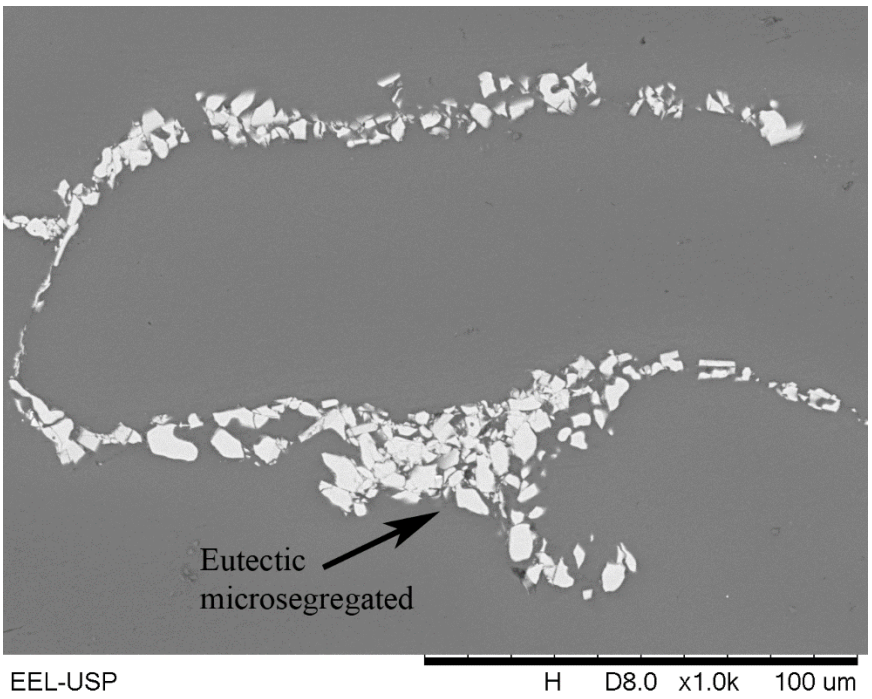

(b)

Figure 4. SEM micrographs of samples after rotary swaging (76% degree of deformation) showing eutectic microsegregation: (a) conventional solidification; (b) vertical upward unidirectional solidification.

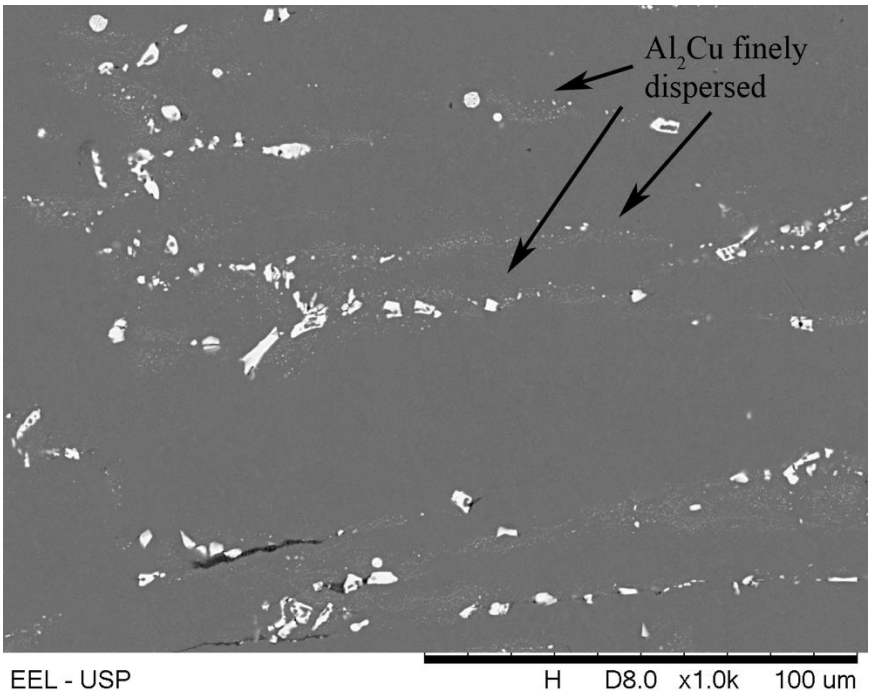

Figure 5. SEM micrograph of Al-4.5 wt.% Cu alloy obtained by conventional solidification, swaged with a deformation degree of 91% and recrystallized at 350 °C for 60 min

Figure 6 presents light optical microscopy (LOM) images of the recrystallized Al-4.5 wt.% Cu alloy obtained by both solidification methods. The alloy obtained by conventional solidification presented a recrystallized microstructure with grains from 40 μm to 50 μm in average size.

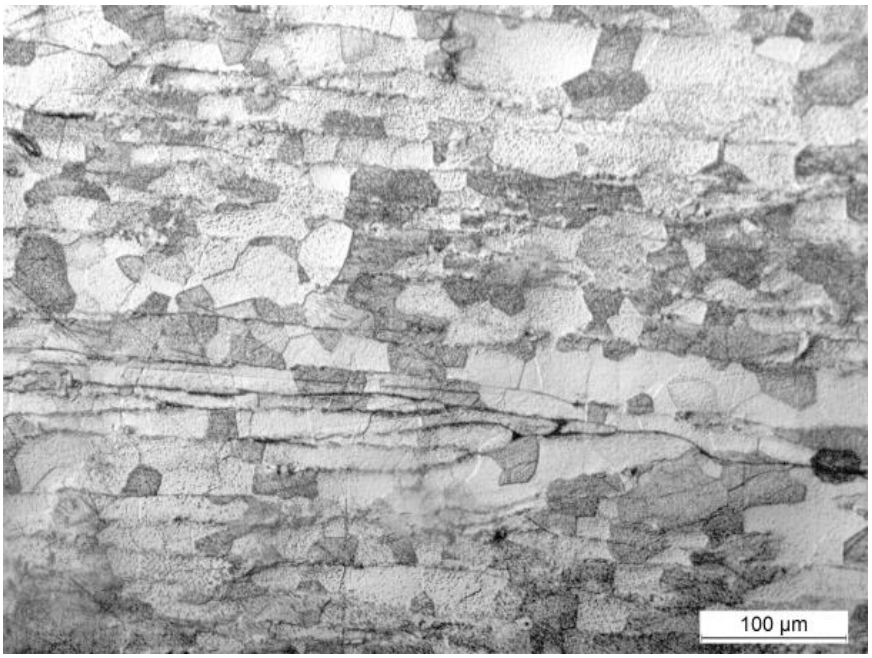

(a)

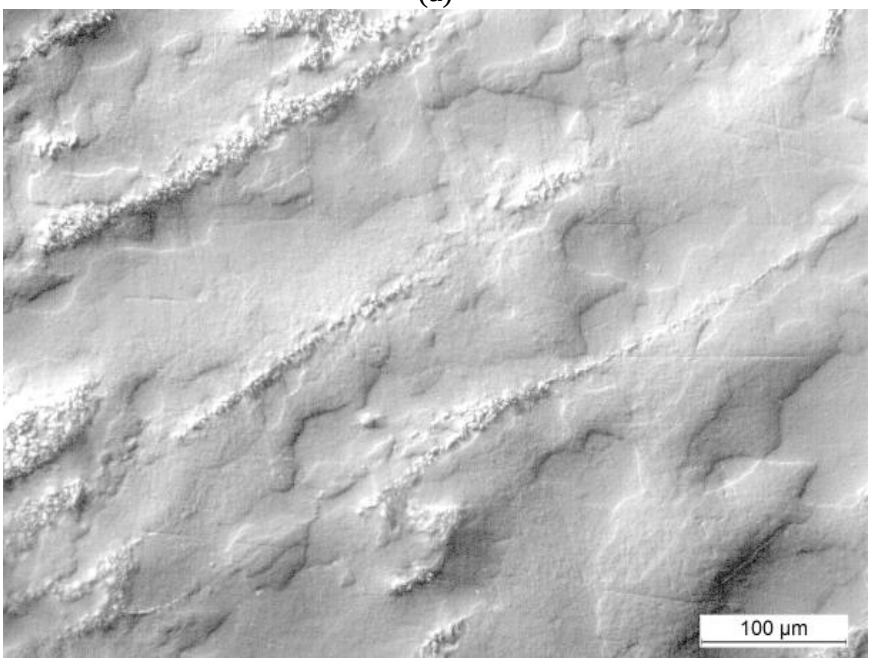

(b)

Figure 6. LOM micrograph of recrystallized Al-4.5 wt.% Cu alloy obtained by (a) conventional solidification; (b) vertical upward unidirectional solidification

The newly recrystallized grains do not entirely follow the deformed microstructure, although the previous elongated grain boundaries generated by the rotary forging process can be identified. The LOM image of the recrystallized alloy obtained by vertical upward unidirectional solidification shows a

coarser microstructure than that obtained by the conventional route. This behavior can be attributed to the microstructure of the alloy obtained by vertical upward unidirectional solidification followed by swaging being coarser and presenting dendrite arm spacing larger than that conventionally solidified and swaged.

As the plastic deformation imposed by rotary forging segregated the eutectic constituent in interdendritic regions, these areas are prone to accumulate great residual tension, which gives extra energy for recrystallization to occur.

As recrystallization heat treatment starts, these sites become active spots for new grain growth. Thus, the conventionally solidified and deformed sample (91% deformation degree) had more prone sites to start the recrystallization process than the other sample, and consequently, it created more new recrystallized grains, resulting in a finer microstructure than the vertical unidirectional upward solidified, deformed and recrystallized sample.

3.2. XRD measurements

3.2.1 Theoretical XRD patterns of Al-4.5 wt.% Cu alloy

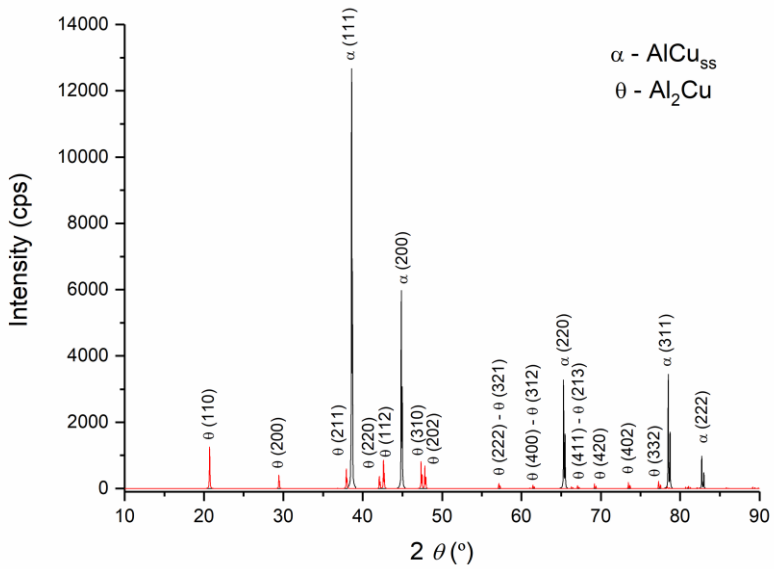

Figure 7. Theoretical X-ray patterns of the Al-4.5 wt%. Cu alloy

The PowderCell and Pearson's Crystal Data.Ink software were used to simulate the theoretical XRD patterns for the Al-4.5 wt.% Cu alloy. This information is necessary to evaluate the orientation index F. Crystallographic data for an α-Al-rich matrix with Cu atoms in substitutional solution (space group N° 225) were applied: a = b = c = 0.40381 nm. For the Al_2Cu secondary phase, crystallographic data were input (space group N° 140): a = b = 0.60670 nm; c = 0.48770 nm. Then, the volume proportion of α-Al/Al_2Cu was adjusted through Al-Cu phase diagram calculus.

This led to the theoretical X-ray patterns of the alloy shown in Figure 7.

Table 2 presents the relative intensity of the ten more intense peaks, five peaks for the α-Al solid solution and five peaks for the Al_2Cu intermetallic phase. The diffractogram patterns of Figure 7 were used to choose the sample whose XRD pattern was the closest to the theoretical pattern. Indeed, the theoretical spectrum cannot be used for the calculation of R_0 since the peaks do not have width; therefore, the integrated intensity cannot be used in equation (1).

Table 2. Data regarding theoretical XRD patterns for Al-4.5 wt.% Cu alloy

2 θ peaks position (°)	**Phase**	**Plane (h k l)**	**Intensity**	**Relative Intensity (%)**
38.59	α-$AlCu_{ss}$	(111)	11863.161	100.00
44.86	α-$AlCu_{ss}$	(200)	5977.994	50.39
78.50	α-$AlCu_{ss}$	(311)	3449.216	29.08
65.30	α-$AlCu_{ss}$	(220)	3278.937	27.64
20.69	Al_2Cu	(110)	1255.38	10.58
82.72	α-$AlCu_{ss}$	(222)	978.285	8.25
42.61	Al_2Cu	(112)	857.502	7.23
47.34	Al_2Cu	(310)	819.224	6.91
47.82	Al_2Cu	(202)	687.453	5.79
37.92	Al_2Cu	(211)	593.37	5.00

Nevertheless, the XRD spectrum of the Al-4.5 wt.% Cu alloy sample, conventionally solidified, deformed by 91% and recrystallized (Figure 8), is very similar to the theoretical X-ray diffractogram (Figure 7). This result is explained by the small, new recrystallized grains, fine microstructure and absence of preferred crystallographic orientations. Thus, the experimental XRD spectrum of this sample was used to obtain the "theoretical" integrated intensities for the α-Al phase and the calculation of R_0 (equation 1).

In general, all XRD spectra presented good peak intensities, and standard deviations between measures (triplicate for each sample) were lower than 5%.

The Lotgering's F index orientation of the Al-4.5 wt.% Cu alloy obtained by conventional solidification and swaging is shown in Figure 9. For the as-cast sample with no plastic deformation, the α-Al phase presents a preferred grain orientation in the (111) direction.

After rotary swaging and a deformation degree of 54%, this preferred orientation disappears, and the grains are randomly oriented. No preferred plane orientation prevails. For a further reduction in area, the grains tend to orient in the (220) direction, and the orientation index increases with the degree of deformation. The (111) planes, which are the densest in the CFC structure, started to suffer rotation with swaging, and the (220) planes became active because plastic deformation continued to occur.

The orientation indexes for Al-4.5 wt.% are shown in Figure 9. The Cu sample with 91% deformation degree and recrystallization is not shown in Figure 9 since its XRD spectrum was chosen as the theoretical spectrum; thus, all its corresponding planes presented an F orientation index equal to 1.

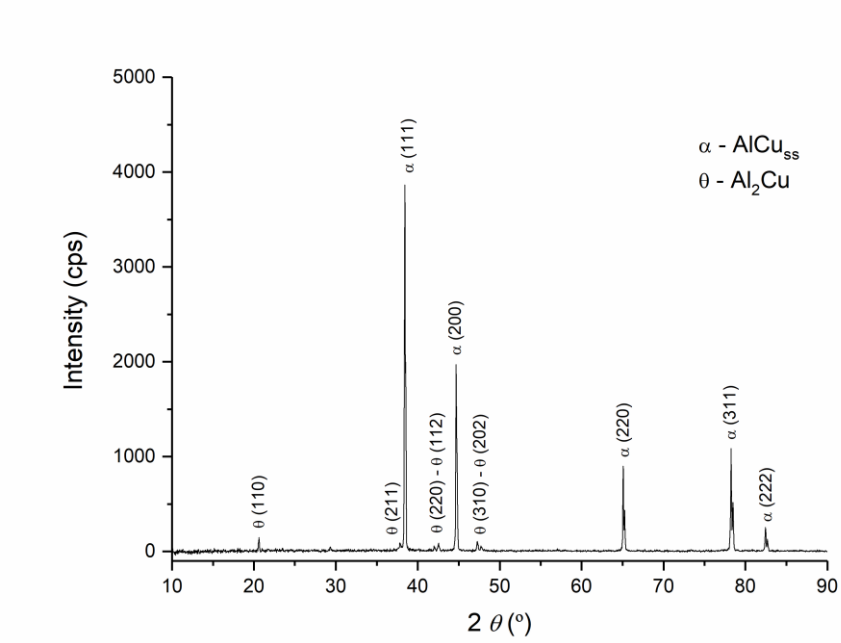

Figure 8. X-ray diffractogram for the Al-4.5 wt.% Cu alloy obtained by conventional solidification, deformed 91% and recrystallized

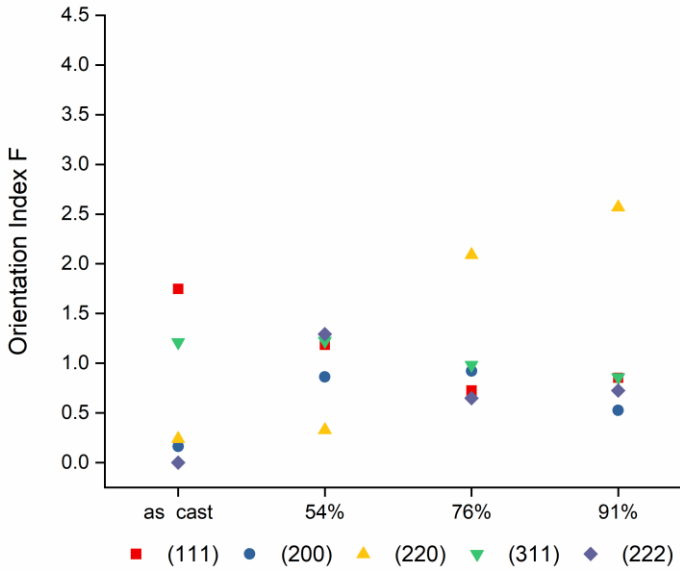

Figure 9. Lotgering's F orientation index for the Al-4.5 wt.% Cu alloy obtained by conventional solidification and swaging with different degrees of deformation

Figure 10 shows the Lotgering's F index orientation for the alloy obtained by unidirectional solidification and swaging. The (200) preferred orientation observed in the as-cast alloy obtained by unidirectional solidification (also observed in Figure 11) tends to gradually disappear with increasing deformation, whereas deformation induces the preferred orientation in the (220) direction (see Figure

12). Although the mode of solidification influenced the orientation of grains in the as-cast alloy, plastic deformation by swaging changed this previous orientation and led to the same (220) preferred orientation in both cases. Recrystallization after deformation also contributed to promoting a similar randomly oriented grain distribution.

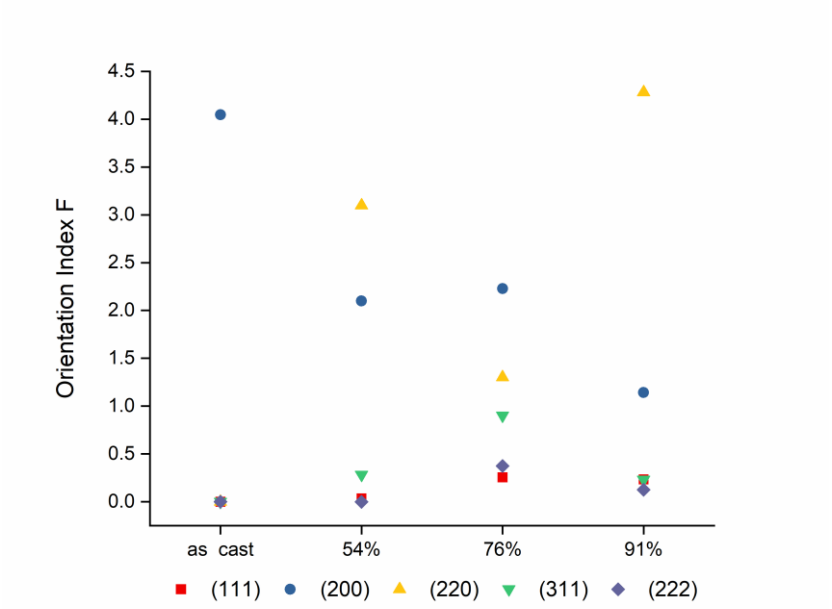

Figure 10. Lotgering's F orientation index for the Al-4.5 wt.% Cu alloy obtained by directional solidification and swaging with different degrees of deformation

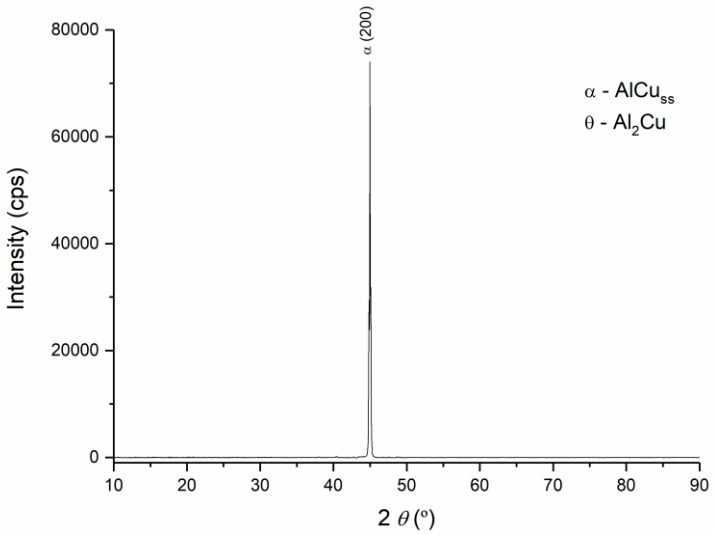

Figure 11. X-ray diffractogram of the as-cast Al-4.5 wt.% Cu alloy obtained by vertical upward unidirectional solidification.

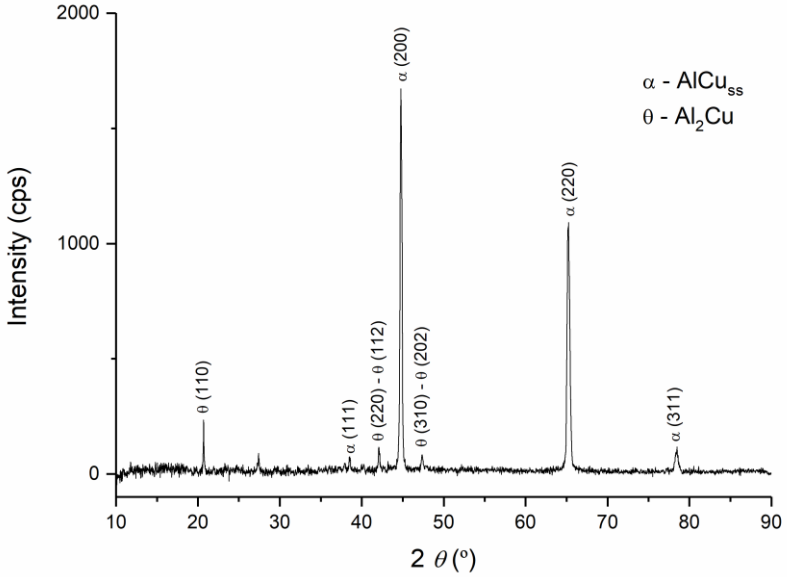

Figure 12. X-ray diffractogram for the Al-4.5 wt.% Cu alloy obtained by vertical upward unidirectional solidification, deformed 54%.

3.3. Electrochemical behavior

Figure 13 shows the open circuit potential (E_{oc}) measurements obtained during 3 h of immersion in 3.5 wt.% NaCl solution for conventionally solidified (Figure 13a) and vertical upward unidirectional solidified (Figure 13b) samples, and E_{oc} values are listed in Table 3. Recrystallized conditions are nobler than others for conventional and unidirectional solidification methods by (30 - 50) mV/SCE, being more positive. These results agree with Chen and collaborators [17], where it was observed in stainless steel that increasing the deformation decreased the equilibrium potentials, indicating that higher deformations lowered the material nobility. As shown in Figure 13, most deformed samples (91% deformation degree) presented lower potentials, whereas recrystallized samples presented the highest potentials due to defect annihilation caused by the recrystallization process. Oscillations of the potential values suggest pitting formation followed by repassivation.

Table 3 also presents the corrosion current density (j_{corr}) and the corrosion potential obtained at the corrosion current density (E_{corr}) for the studied conditions obtained by Tafel extrapolation using the polarization curves (Figures 14a and 14b). For the as-cast and 54% deformed conditions, the corrosion current density is lower for conventionally solidified samples than for the unidirectionally solidified samples. For higher deformation degrees (76%, 91% and 91% RC), the unidirectionally solidified samples presented lower corrosion current densities than the conventional samples.

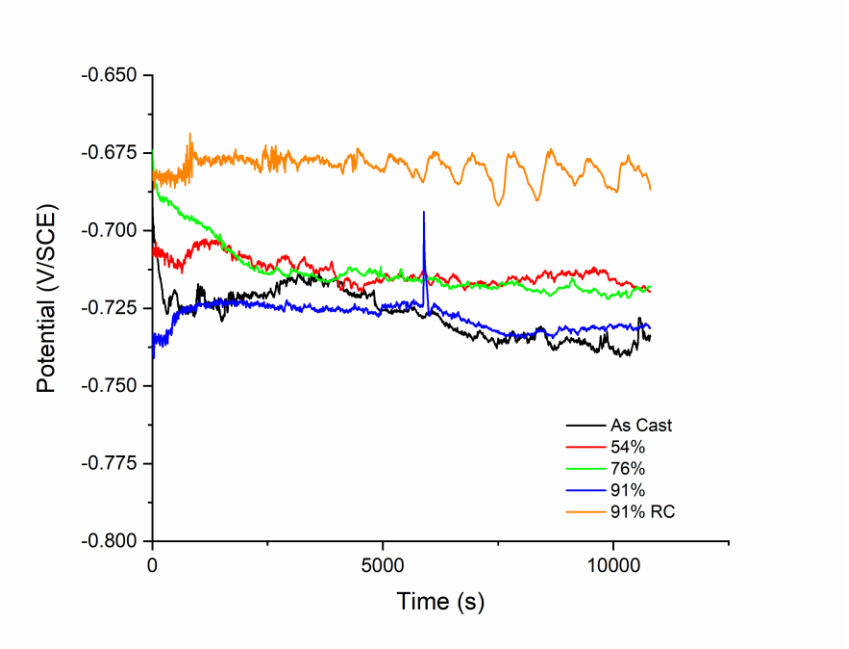

(a) conventional solidification

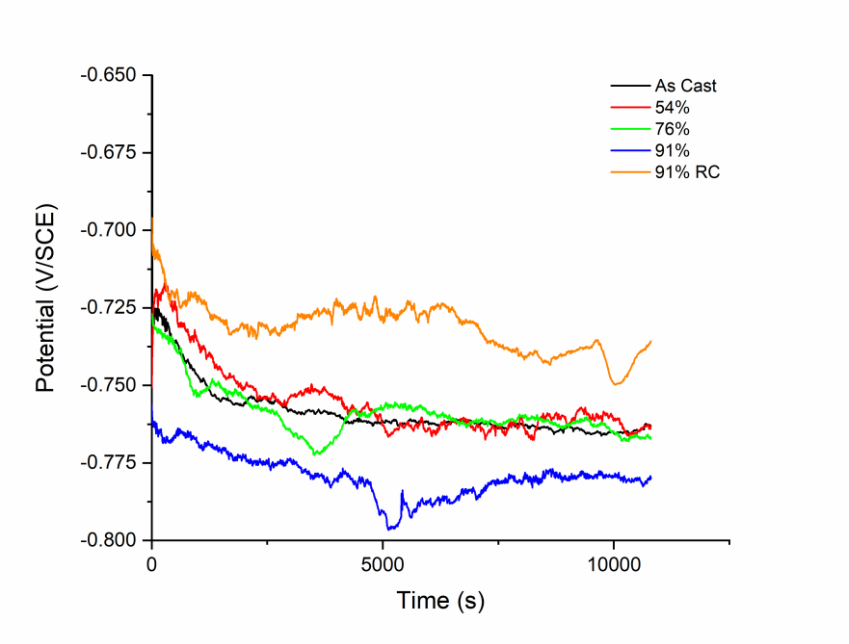

(b) vertical upward unidirectional solidification

Figure 13. Open circuit potential measurements obtained during 3 h of immersion in 3.5 wt.% NaCl solution for the investigated Al-4.5 wt.% Cu alloy under different solidification conditions: (a) conventional; (b) vertical upward unidirectional

Table 3. Electrochemical parameters obtained in 3.5 wt.% NaCl solution for the investigated Al-4.5 wt.% Cu alloy: open circuit potential (E_{oc}) after 3 h of immersion; corrosion potential (E_{corr}) and corrosion current density (j_{corr}) obtained via the Tafel slope extrapolation method

	E_{oc} t = 3 h (V/SCE)		E_{corr} (V/SCE)		j_{corr} ($\mu A.cm^{-2}$)	
Samples	Conventional	Vertical upward unidirectional	Conventional	Vertical upward unidirectional	Conventional	Vertical upward unidirectional
as-cast	-0.734	-0.763	-0.632	-0.667	2.86	3.16
54%	-0.719	-0.763	-0.664	-0.704	0.91	3.30
76%	-0.718	-0.767	-0.632	-0.712	8.74	4.34
91%	-0.731	-0.779	-0.664	-0.714	7.70	4.85
91% RC	-0.686	-0.736	-0.635	-0.674	6.42	5.70

Potentiodynamic polarization curves in 3.5 wt.% NaCl solution were performed to study the corrosion behavior of the Al-4.5 wt.% Cu alloy obtained under different conditions.

Figure 14 shows the potentiodynamic polarization curves for conventional (Figure 14a) and vertical upward unidirectional (Figure 14b) samples.

In the anodic region, a linear potential region was observed, suggesting activity on the surface of the samples, as shown in Figure 14. The main reaction in this medium is:

$Al \rightarrow Al^{3+} + 3e^-$

The cathodic polarization part of the curves suggests oxygen reduction,

$O_2 + 2H_2O + 4e^- \rightarrow 4OH^-$

followed by water reduction:

$2H_2O + 2e^- \rightarrow H_2 + 2OH^-$

The strong similarity of the corrosion potentials of the investigated samples is also verified.

The Bode plots (impedance modulus vs. frequency and phase angles vs. frequency) are shown in Figure 15 for conventional (Figure 15a) and unidirectional (Figure 15b) samples, and impedance modulus values at low frequency are given in Table 4.

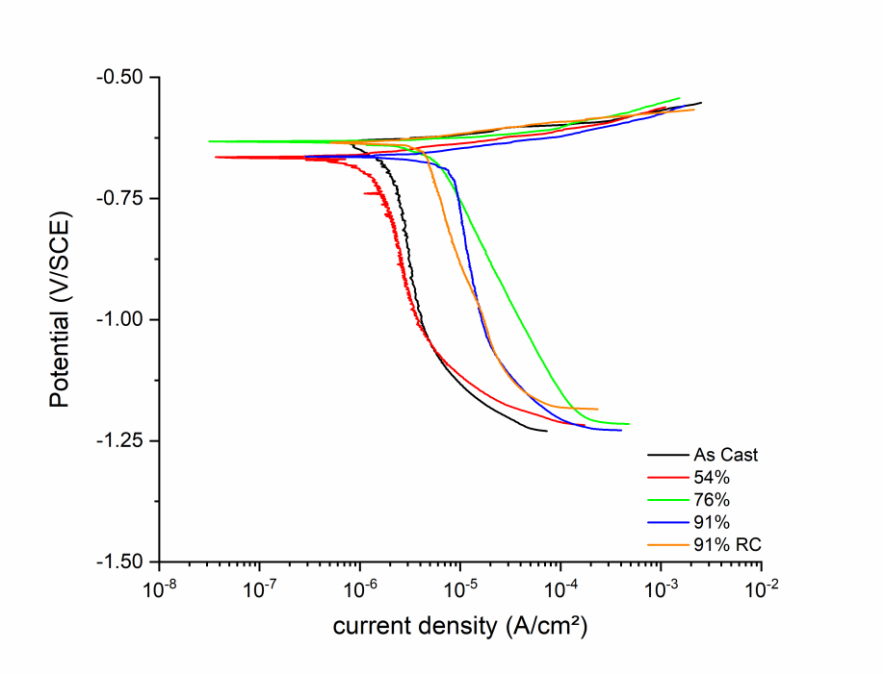

(a) conventional

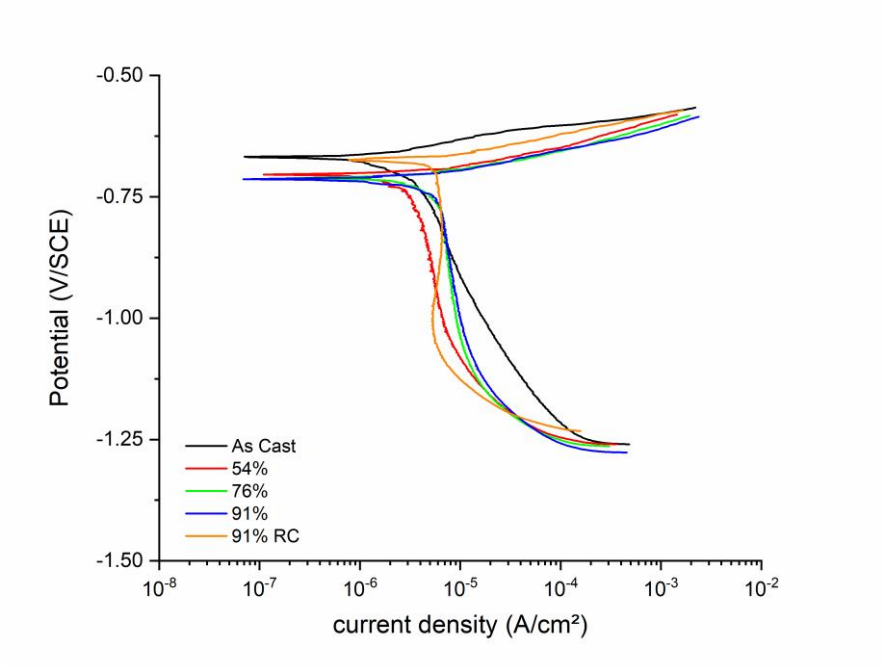

(b) vertical upward unidirectional

Figure 14. Potentiodynamic polarization curves obtained in 3.5 wt.% NaCl solution for the investigated Al-4.5 wt.% Cu alloy under different solidification conditions: (a) conventional; (b) vertical upward unidirectional

The impedance modulus at low frequency is an indirect indicator of the corrosion resistance, in which a higher impedance modulus at low frequency means higher corrosion resistance, as its values

represent an outer oxide film [18]. This measurement is considered a reliable way to evaluate the corrosion resistance because EIS measurements disturb the system at very small potential amplitudes. The impedance modulus at low-frequency values is discussed in this text in terms of comparing the corrosion resistance of the studied conditions.

In Figure 15a, a higher impedance modulus at low frequency is obtained for the as-cast condition and the 54% degree of deformation samples. A lower impedance modulus at low frequency is observed for even higher deformations. These observations were made by Alain et al. [8], who attributed these differences to defects in the material (dislocations) and possible stored residual stresses, increasing the available electron activity for electrochemical reactions. The condition of 91% deformed and recrystallized presented a higher impedance modulus at low frequency than samples with 76% and 91% of deformation degree, which is attributed to the recrystallization process that annihilates surface defects and residual stresses [9]. For conventionally solidified samples, the phase angle shows a single peak, which is commonly observed in active corrosion mechanisms.

In the unidirectional solidified samples (Figure 15b), a higher impedance modulus at low frequency is obtained for the 91% deformed and recrystallized sample, followed by the 54% deformed sample. In this case, a similar behavior to the conventional samples is observed for samples with 76% and 91% deformation degrees, in which the impedance modulus at low frequency (0.01 Hz) decreased with the increase in plastic deformation by the rotary swaging process. The as-cast sample presented a lower impedance modulus at low frequency than the samples with 54% and 76% deformation, which differed from the conventionally solidified condition. The phase angles for unidirectional samples are also a single peak, as in the conventional solidified samples, except for the as-cast sample, which presented a different behavior, with two peaks present.

Relating the EIS results with the XRD results, the unidirectional as-cast condition, which presented only the (200) crystallographic peak, presented a lower impedance modulus at low frequency and different phase angle behavior. After rotary swaging plastic forming, at 54% degree of deformation, other crystallographic planes appeared, increasing the impedance modulus at low frequency, meaning that corrosion resistance was improved. This result is strong evidence that in this case, not only did the residual stresses and surface defects due to deformation play an important role in decreasing the corrosion resistance but also the changes in the crystallographic planes affected the final corrosion resistance of this alloy. As deformation increased, (220) less dense crystallographic planes appeared, as more residual stresses from deformation decreased the impedance modulus at low frequency, leading to lower corrosion resistance. Recrystallized samples then presented new grains with lower residual stress in the lattice and lower surface defects along with a new crystallographic peak pattern, improving corrosion resistance again.

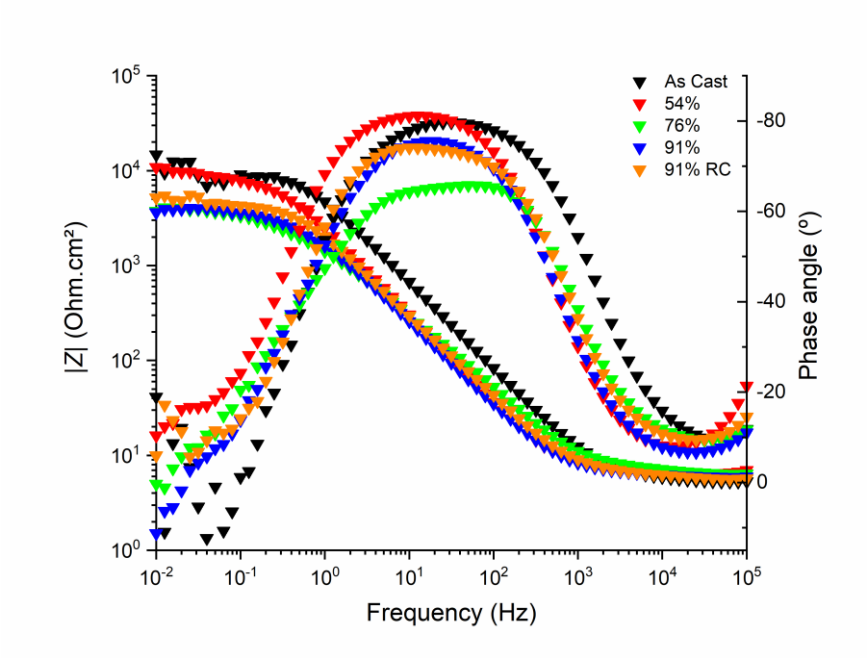

(a) conventional

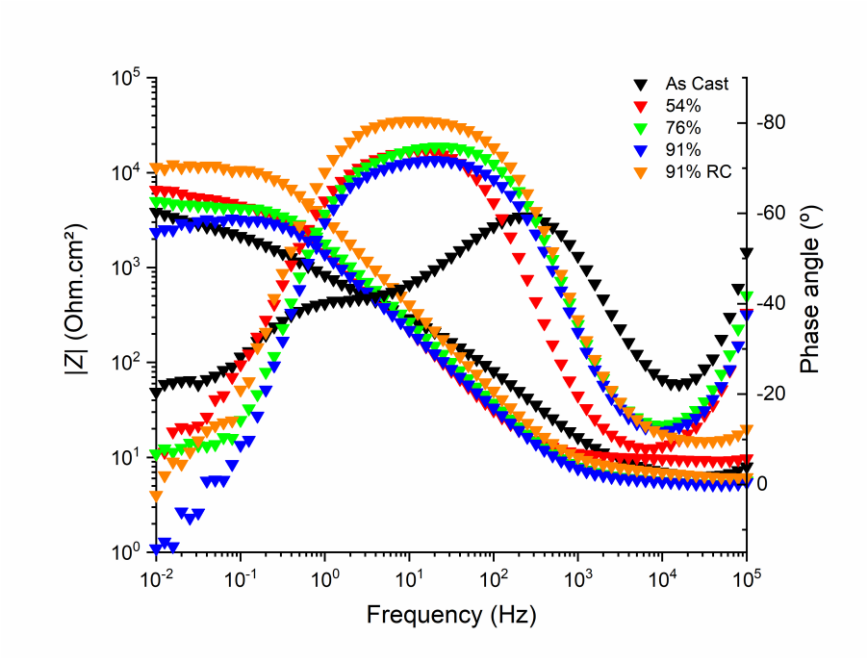

(b) vertical upward unidirectional

Figure 15. Bode diagram and phase angle obtained in a 3.5 wt.% NaCl solution for the investigated Al-4.5 wt.% Cu alloy under different solidification conditions: (a) conventional; (b) vertical upward unidirectional

Table 4. Impedance modulus values measured at 0.01 Hz for the investigated Al-4.5 wt.% Cu alloy under different solidification conditions

Samples	|*Z*| at 0.01 Hz (Ω.cm²)	
	Conventional	Vertical upward unidirectional
as-cast	14767	3845
54%	10893	6569
76%	3760	4999
91%	3632	2363
91% RC	5191	11456

4. CONCLUSIONS

The microstructure of the Al-4.5 wt.% Cu alloy was composed of an α-Al aluminum-rich phase with copper substitutional atoms present in solid solution and a secondary Al_2Cu phase present in the form of a eutectic at interdendritic regions.

The microstructure of the as-cast Al-4.5Cu wt.% alloy obtained by conventional solidification presented an equiaxed morphology, whereas the microstructure obtained by unidirectional solidification was columnar.

Rotary swaging alloys with deformation degrees of 54%, 76% and 91% led to gradual grain elongation, a decrease in interdendritic arm spacing and eutectic microsegregation.

Heat treatment at 350 °C for 60 min on alloy produced by both solidification routes and posteriorly deformed 91% promoted the recrystallization process, creating a new equiaxed microstructure.

The as-cast Al-4.5%wt. Cu alloys obtained by conventional and unidirectional solidification routes presented the (111) and (200) preferred orientations, respectively.

These preferred orientations gradually disappeared with plastic forming by rotary swaging, which was changed to the (220) preferred orientation in both cases as the deformation increased.

A randomly oriented grain microstructure was obtained after recrystallization treatment.

Conventional and unidirectional 91% AR-recrystallized samples presented higher values of final OCP, meaning higher nobility than other studied conditions.

Under conventionally solidified conditions, the rotary swaging process decreased the corrosion resistance of the Al-4.5 wt.% Cu alloy. Higher deformations led to lower corrosion resistance (observed by the impedance modulus at low frequency). The Al-4.5 wt.% Cu 91% recrystallized condition presented an increase in the impedance modulus at low frequency, which was attributed to new grains randomly oriented exempt of surface defects and residual stresses. The highest impedance modulus at low frequency is obtained for Al-4.5 wt.% Cu in the as-cast condition.

For the unidirectionally solidified samples, the cast condition presented a lower impedance modulus at low frequency than conventionally solidified cast Al-4.5 wt.% Cu. The rotary swaged sample with 54% deformation presented a higher impedance modulus at low frequency, and higher deformations

(76% and 91%) presented a lower impedance modulus at low frequency. The recrystallized sample in this solidification method presented the highest impedance modulus at low frequency for this condition.

CONFLICT OF INTEREST
The authors declare that they have no conflicts of interest.

ACKNOWLEDGEMENTS
This study was financed in part by the Coordenação de Aperfeiçoamento de Pessoal de Nível Superior - Brasil (CAPES) - Finance Code 001.

References

1. J.L. Murray, H. Baker, H. Okamoto, S.D. Henry, G.M. Davidson, M.A. Fleming, L. Kacprzak, ASM Handbook: Alloy Phase Diagram, 1ª ed., ASM International, (n.d.) United States of America.
2. L.J. Korb, D.L. Olson, ASM Handbook: Corrosion, 4ª ed, ASM International, (1992) United States of America.
3. S. Henry, T. Minghetti, M. Rappaz, *Acta Mater.*, 46 (1998) 6431–6443.
4. F.Y. Xie, T. Kraft, Y. Zuo, C.H. Moon, Y.A. Chang, *Acta Mater.*, 47 (1999) 489–500.
5. D. Eskin, Q. Du, D. Ruvalcaba, L. Katgerman, *Mater. Sci. Eng. a-Structural Mater. Prop. Microstruct. Process.*, 405 (2005) 1–10.
6. W.R. Osorio, J.E. Spinelli, C.M. Freire, A. Garcia, *Mater. Sci. Technol.*, 24 (2008) 1433–1437.
7. W.R. Osorio, J.E. Spinelli, C.M.A. Freire, M.B. Cardona, A. Garcia, *J. Alloys Compd.*, 443 (2007) 87–93.
8. A. Robin, G.A. Santana Martinez, P.A. Suzuki, *Mater. Des.*, 34 (2012) 319–324.
9. A.F. Padilha, F.S. Junior, Encruamento, Recristalização, Crescimento de Grão e Textura, 3ª ed., ABM - Associação Brasileira de Metalurgia e Materiais, (2005) São Paulo.
10. O. Engler, X.W. Kong, K. Lucke, *Scr. Mater.*, 41 (1999) 493–503.
11. O. Engler, X.W. Kong, K. Lucke, *Acta Mater.*, 49 (2001) 1701–1715.
12. M. Abdulstaar, M. Mhaede, L. Wagner, M. Wollmann, *Mater. Des.*, 57 (2014) 325–329.
13. R.A.G. Matos, Estudo Comparativo Da Recristalização Da Liga Al-4.5Cu Após Forjamento Rotativo, Obtida Por Solidificação Convencional e Unidirecional, Universidade Federal de Itajubá, 2014.
14. F.K. Lotgering, *J. Inorg. Nucl. Chem.*, 9 (1959) 113.
15. W.R. Osorio, J.E. Spinelli, I.L. Ferreira, A. Garcia, *Electrochim. Acta*, 52 (2007) 3265–3273.
16. W.D. Callister, D.G.C.N.-S.M.L. Rethwisch Stacks, LC Classification TA403 .C23 2010 (LC), Materials Science and Engineering : An Introduction, 8th ed., John Wiley & Sons, (2010) Hoboken, NJ.
17. X. Chen, M. Gussev, M. Balonis, M. Bauchy, G. Sant, *Mater. Des.*, 203 (2021).
18. Y. Wu, W. Zhao, Z. Lu, L. Wang, *Carbon N. Y.*, 179 (2021) 445–457.

© 2021 The Authors. Published by ESG (www.electrochemsci.org). This article is an open access article distributed under the terms and conditions of the Creative Commons Attribution license (http://creativecommons.org/licenses/by/4.0/).